Eur. Phys. J. B (2012) 85: 376
DOI: 10.1140/epjb/e2012-30398-1

THE EUROPEAN PHYSICAL JOURNAL B

Regular Article

Evolution of quantum strategies on a small-world network

Q. Li[1,2,a], A. Iqbal[2], M. Chen[1], and D. Abbott[2]

[1] College of Electrical Engineering, Chongqing University, Chongqing 400030, P.R. China
[2] School of Electrical and Electronic Engineering, University of Adelaide, SA 5005, Australia

Received 19 May 2012 / Received in final form 23 September 2012
Published online 19 November 2012 –

Abstract. In this paper, quantum strategies are introduced within evolutionary games in order to investigate the evolution of quantum strategies on a small-world network. Initially, certain quantum strategies are taken from the full quantum space at random and assigned to the agents who occupy the nodes of the network. Then, they play n-person quantum games with their neighbors according to the physical model of a quantum game. After the games are repeated a large number of times, a quantum strategy becomes the dominant strategy in the population, which is played by the majority of agents. However, if the number of strategies is increased, while the total number of agents remains constant, the dominant strategy almost disappears in the population because of an adverse environment, such as low fractions of agents with different strategies. On the contrary, if the total number of agents rises with the increase of the number of strategies, the dominant strategy re-emerges in the population. In addition, from results of the evolution, it can be found that the fractions of agents with the dominant strategy in the population decrease with the increase of the number of agents n in a n-person game independent of which game is employed. If both classical and quantum strategies evolve on the network, a quantum strategy can outperform the classical ones and prevail in the population.

1 Introduction

Recently, the evolution of agents' behavior in a population, in the framework of the evolutionary games on networks, has attracted much interdisciplinary attention. As complex network theory developed, a shift from evolutionary games on regular lattices to evolutionary games on complex networks was observed [1], in particular on small world networks [2–7]. Moreover, the two-person Prisoner's Dilemma (PD) and Snowdrift (SD) games have been widely studied. However, some situations such as collective actions of groups of individuals cannot be abstracted appropriately by two-person games. Therefore, n-person games as the generalization of two-person games offer new models for study of the collective behavior of interacting agents. For a $n \times m$ game, each of n agents chooses a strategy from m strategies simultaneously, and then each receives a payoff according to a payoff matrix of the game. Interesting results have been obtained for n-person games [8–11]. For example, Eriksson and Lindgren [8] investigated the cooperation driven by mutations when n-person PD games were employed; Chan et al. [9] reported results regarding the evolution of cooperation in a well-mixed population performing n-person SD games.

Surprisingly, the concept of evolutionary games has been extended to the microworld to describe interactions of biological molecules [12–15], a domain in which quantum mechanics defines the laws. In recent years, the new field of quantum game theory has emerged as the generalization of classical game theory. Due to quantum effects involved, quantum games exhibit new features that have no classical counterparts and it opens up new lines of research. For example, Meyer [16] first quantized the PQ penny flip game. His results showed that when an agent implements quantum strategy against the opponent's classical strategy, she/he can always defeat her/him and can thus increase her/his expected payoff. Eisert et al. [17] introduced an elegant scheme to quantize the PD game and demonstrated that the dilemma in the classical PD could be escaped when both agents resort to quantum strategies. Marinatto and Weber [18] gave a quantum model of the Battle of the Sexes game and found a unique Nash equilibrium (NE) for this game, when the entangled strategies were allowed, whereas the classical game has two NEs. Later, Iqbal and Toor [19] studied evolutionarily stable strategies in quantum games and Kay et al. [20] presented an evolutionary quantum game. Moreover, quantum games were implemented using quantum computers [21–23] and some related researches have also been performed [24–28]. For further background on quantum games, see references [29,30].

Additionally, in order to study the evolving behavior of agents in a population, a framework is often used [2–6], in which agents in the population are regarded as nodes

[a] e-mail: anjuh@cqu.edu.cn

and the relationships between them as links. As such, a network representing the relationships of agents is created. Then, these connected agents will interact with each other by using different strategies, and certain patterns emerge in the population after a large number of interactions. Because of the diversities of agents' behavior and interactions, a large strategy space is needed to describe their behavior in a large population. Fortunately, the full quantum strategy space turns out to be a very large space, i.e., the classical strategy space is only a subset of the quantum one, in which each agent can behave according to a given strategy. However, agents using strategies in the full quantum strategy space must resort to quantum games to interact with other agents.

In this paper, we focus on investigating the evolution of quantum strategies on a small-world network based on the physical model of a quantum game. The small-world network is a type of complex networks that exhibits some features of social networks in real world, such as the short average path length and the large clustering coefficient. After the network is established, all nodes on the network are occupied by agents and they play $n \times m$ quantum games with their neighbors. The main difference between the quantum and the classical game is that certain quantum effects, such as entanglement, are involved, which also bring new results that have no classical counterparts. Agents' actions are performed on a quantum superposition state that contains all possible results before measurement. If the superposition state is measured, it will collapse to one of the states in the superposition with certain probability. After the interactions of agents are carried out a large number of times, new patterns emerge in the population. Later, how the evolution of strategies is influenced by different parameters is analyzed and discussed, when two n-person games are employed. Furthermore, after two classical strategies are selected from the full quantum strategy space, the evolution of quantum and classical strategies on the network is studied. It is worth noting that a quantum strategy is not a probabilistic sum of pure classical strategies (except under special conditions), and then it cannot be reduced to the pure classical strategies [19].

The rest of this paper is organized as follows. Section 2 briefly introduces the physical model of a n-person quantum game. Next, the model for the evolution is described in Section 3. In Section 4, the results of the evolution are given first and then they are explained in detail by analyzing the data. Next, the relationships between the results and different parameters are discussed, when two n-person games are adopted. The conclusion is given in Section 5.

2 n-Person quantum games

Before introducing quantum games, some basic concepts of quantum computation are introduced here. The elementary unit in quantum computation is called the qubit, which is typically a microscopic system. Moreover, the Boolean states 0 and 1 are represented by a prescribed pair of normalized and mutually orthogonal quantum states labeled as $\{|0\rangle, |1\rangle\}$ to form a 'computational basis' [31]. Any pure state of the qubit can be written as a superposition state $\alpha|0\rangle + \beta|1\rangle$ for some α and $\beta \in C$ satisfying $|\alpha|^2 + |\beta|^2 = 1$ [31]. Any manipulations on qubits have to be performed by unitary operations, which can be undertaken by a quantum logic gate or a quantum circuit [31]. Suppose that there is a quantum register with n qubits, by which 2^n states can be represented simultaneously. If the register is operated by a quantum circuit, 2^n results can be computed simultaneously by one unitary operation, whereas classically these results need to be computed one by one. Therefore, a number of classical problems can be solved with a speed-up in the quantum world. For example, the Deutsch-Jozsa algorithm [32] can determine whether a function is constant or balanced by one operation, whereas a classical algorithm needs $2^{n-1} + 1$ in the worst case. For further details, see references [31,33].

As is known, the PD and SD games are widely applied in a number of scientific fields. For a classical 2×2 game, each agent has two available strategies, Cooperation (C) and Defection (D). Agents choose their strategies independently. Finally, each agent receives a payoff that depends on the selected strategies, where the payoff matrix to the first (or focal) agent can be written as

$$\begin{array}{c} \\ C \\ D \end{array} \begin{array}{c} \begin{array}{cc} C & D \end{array} \\ \begin{pmatrix} R & S \\ T & P \end{pmatrix} \end{array}. \tag{1}$$

If both agents are cooperators or defectors, they receive R (Reward) or P (Punishment). If one is a cooperator and the other is a defector, the cooperator receives S (Sucker), while the defector receives T (Temptation). As an extension of a two-person game, a n-person game is more complex, in which the first agent plays the game with other $n-1$ agents. Then, the payoff of the first agent can be calculated as follows, according to its strategy and the number of cooperators in a n-person game [8,9]:

PD:

$$P_i = \begin{cases} P_C(n_c) = \dfrac{n_c}{n-1}, & \text{if Strategy } C \\ P_D(n_c) = T\dfrac{n_c}{n-1} + P\dfrac{n-n_c-1}{n-1}, & \text{if Strategy } D, \end{cases} \tag{2}$$

SD:

$$P_i = \begin{cases} 1 - \dfrac{r}{n_c}, & \text{if Strategy } C \\ 0, & \text{if Strategy } D \text{ and } n_c = 0 \\ 1, & \text{if Strategy } D \text{ and } n_c > 0. \end{cases} \tag{3}$$

Here, n_c is the number of cooperators in a n-person SD game, but in a n-person PD game, it is the number of cooperators not including the first agent, if the first agent is a cooperator. In the SD game, the cost-to-benefit ratio is defined as $r = c/b$, where c is the total cost to shovel the snowdrift, while b is the benefit for each agent.

In the following part, the n-person quantum game [34] will be introduced briefly, which is a generalization of a two-person quantum game [17]. The physical model of a

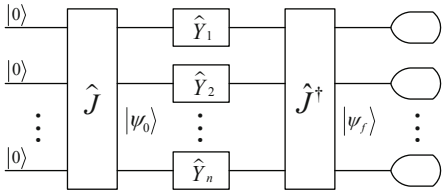

Fig. 1. The physical model of a n-person quantum game.

n-person quantum game is shown in Figure 1, in which the possible outcomes of the classical strategies, $C = 0$ and $D = 1$, are assigned to two basis vectors $\{|C = 0\rangle, |D = 1\rangle\}$ in Hilbert space, respectively.

Assume that the initial state of a n-person game is $|\psi_0\rangle = \hat{J}\,|\underbrace{0\ldots0}_{n}\rangle$, where $\hat{J}$ is an entangling operator that is known to n agents. For the n-person quantum game, the general form of $\hat{J}$ can be written as [34,35]

$$\hat{J}(\gamma) = \exp\left(i\frac{\gamma}{2}\sigma_x^{\otimes n}\right) = I^{\otimes n}\cos\frac{\gamma}{2} + i\sigma_x^{\otimes n}\sin\frac{\gamma}{2}, \quad (4)$$

where $\gamma \in [0, \pi/2]$ is a measure of entanglement of a game. When $\gamma = \pi/2$, there is a maximally entangled game, in which the entangling operator takes the following form:

$$\hat{J}(\gamma) = \frac{1}{\sqrt{2}}\left(I^{\otimes n} + i\sigma_x^{\otimes n}\right). \quad (5)$$

Next, each agent chooses a unitary operator $\hat{Y}$ as a strategy from the full quantum strategy space $\hat{S}$ [29],

$$\hat{Y}(\alpha,\beta,\theta) = \begin{pmatrix} e^{i\alpha}\cos\frac{\theta}{2} & ie^{i\beta}\sin\frac{\theta}{2} \\ ie^{-i\beta}\sin\frac{\theta}{2} & e^{-i\alpha}\cos\frac{\theta}{2} \end{pmatrix} \in \hat{S}, \quad (6)$$

where $\alpha, \beta \in [-\pi, \pi]$, $\theta \in [0, \pi]$, and operates it upon the qubit that belongs to her/him, which puts the game in a state $(\hat{Y_1} \otimes \ldots \otimes \hat{Y_n})\hat{J}|\underbrace{0\ldots0}_{n}\rangle$.

In the end, before a projective measurement on the $\{|0\rangle, |1\rangle\}$ basis is carried out, the final state is

$$|\psi_f\rangle = \hat{J}^\dagger\left(\hat{Y_1} \otimes \ldots \otimes \hat{Y_n}\right)\hat{J}\,|\underbrace{0\ldots0}_{n}\rangle. \quad (7)$$

Thus, the first agent's expected payoff has the following form

$$\begin{aligned} \Pi(\hat{Y_1},\ldots,\hat{Y_n}) = {} & P(|\underbrace{0\ldots0}_{n}\rangle)|\langle\underbrace{0\ldots0}_{n}|\psi_f\rangle|^2 \\ & + P(|\underbrace{0\ldots1}_{n}\rangle)|\langle\underbrace{0\ldots1}_{n}|\psi_f\rangle|^2 + \ldots \\ & + P(|\underbrace{1\ldots1}_{n}\rangle)|\langle\underbrace{1\ldots1}_{n}|\psi_f\rangle|^2, \end{aligned} \quad (8)$$

while the measured payoff is

$$\Pi(\hat{Y_1},\ldots,\hat{Y_n}) = P(M(|\psi_f\rangle)), \quad (9)$$

where $M(\cdot)$ is the measurement function. If the final state $|\psi_f\rangle$ is measured, it will collapse to a state in the superposition with certain probability. Here, $|\langle\cdot|\psi_f\rangle|^2$ is the probability when the final state $|\psi_f\rangle$ collapses to the state $|\cdot\rangle = M(|\psi_f\rangle)$, while $P(|\cdot\rangle)$ denotes the first agent's payoff under the strategy profile corresponding to that state. For example, $P(|\underbrace{0\ldots1}_{n}\rangle)$ represents the first agent's payoff when the final state collapses to the state $|\underbrace{0\ldots1}_{n}\rangle$, where it plays the strategy C and other agents also plays the strategy C except the last agent uses the strategy D.

3 The model

Assume that there is an undirected small-world network $G(V, E)$ with N nodes, where V is the set of nodes and E is the set of links. For avoiding isolated nodes, the Newman-Watts (NW) small-world network [36,37] is selected in this paper instead of the Watts-Strogatz (WS) network. The NW network can be established in the following ways [38]. At first, a one-dimensional lattice with periodic boundary conditions is constructed, in which each node is connected to $k_{\rm nn}$ nearest neighbors, and then links are added with probability $p_{\rm nw}$ between any two randomly chosen nodes. Also, each node $i \in V$ is occupied by an agent and its neighbor j is any other agent such that there is a link between them, so the set of neighbors of an agent i can be defined as $\Gamma_i = \{j|e_{ij} \in E, j \in V \setminus i\}$ and the number of neighbors is $k = |\Gamma_i|, k \geq k_{\rm nn}$, where $V \setminus i$ means the set of nodes, V, not including the ith node (a complement of $\{i\}$ in V) and $|\cdot|$ is the cardinality of a set.

Next, m strategies are randomly taken from the full quantum strategy space $\hat{S}$ by choosing the parameters, α, β and θ, in equation (6) at random before each simulation starts. Then, they are assigned to agents on the network at random with equal probability. Later, a randomly selected agent i play $n \times m$ $(n, m \geq 2)$ maximally entangled quantum games with its neighbors according to the physical model of a quantum game (Fig. 1). Because n-person games are employed, neighbors of the agent are randomly divided into $l = \lceil k/(n-1)\rceil$ groups before games are played, where $l \geq 1$ is satisfied and the symbol $\lceil\cdot\rceil$ indicates the integral part of a number. The number of neighbors k is not necessarily an integer multiple of $n-1$, if $\lceil\cdot\rceil$ is applied. For the $k - l(n-1)$ remaining neighbors, they are omitted from the current round. Later, the first agent plays games in turn with $n-1$ neighbors in each of l groups in terms of the physical model, and its payoff $\Pi(\hat{Y_1},\ldots,\hat{Y_n})$ can be calculated by equation (8) or equation (9). The agent's total payoff F_i is obtained by accumulating all it receives, $F_i = \sum_l \Pi_l(\hat{Y_1},\ldots,\hat{Y_n})$.

After these, a neighbor $j \in \Gamma_i$ is chosen at random from the agent i's neighborhood and its payoff F_j is also calculated according to the above mentioned method. The agent i will imitate this neighbor's strategy with

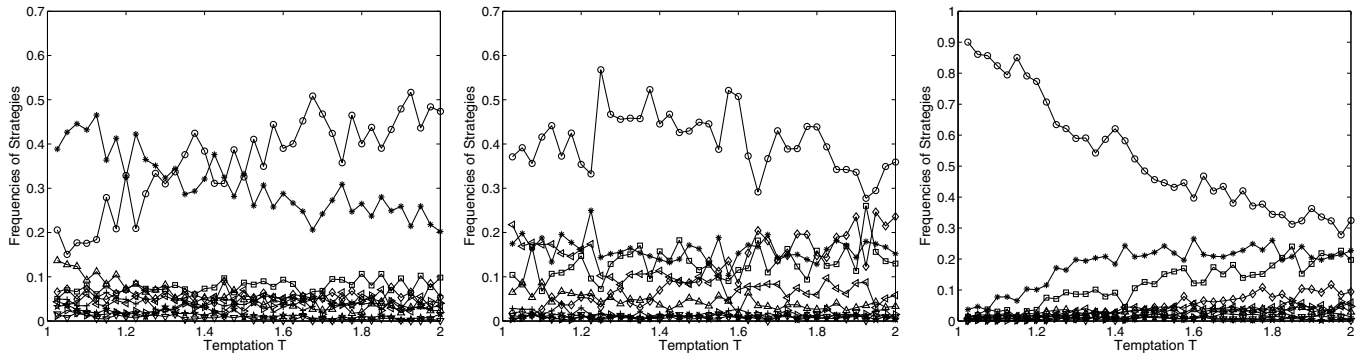

Fig. 2. The evolution of strategies when different initial strategies are selected. (a) $h = 1$, (b) $h = 2$ and (c) $h = 3$. They are drawn according to three $\omega_h(T), h = 1, 2, 3, T \in (1, 2]$, which are obtained from three groups of initial strategies in a population of $N = 2\,500$ agents after $50\,000$ generations, when the 2×10 ($n = 2, m = 10$) Prisoner's Dilemma (PD) games are employed. Each group of initial strategies includes $m = 10$ quantum strategies $\hat{Y}(\alpha, \beta, \theta)$ that are selected by randomly choosing the parameters $\alpha, \beta \in [-\pi, \pi]$, $\theta \in [0, \pi]$, before a simulation starts, so there are ten curves $\omega_h(T, m), T \in (1, 2], m = 1, 2, \ldots, 10$ in each graph.

probability p_i [39],

$$p_i = \frac{1}{1 + e^{(F_i/l_i - F_j/l_j)/\lambda}}, \tag{10}$$

where l_i and l_j are the numbers of groups, into which the neighbors of the agent i and j are divided, respectively, and the variable λ is the intensity of selection. If the agent i decides to imitate this strategy, it will update its strategy and apply it in the next round.

This whole process is iterated for a maximum number of 5×10^4 generations, and the fractions of agents with different strategies are obtained by averaging another 1000 generations after the maximum. Thus, a result of evolution of strategies for a simulation is produced, $\omega_h(\epsilon) = \{\omega_h(\epsilon, Q_1), \ldots, \omega_h(\epsilon, Q_m)\}$, $\epsilon = T$ or r, where $\omega_h(\epsilon, Q_m)$ denotes the fraction of agents with the mth strategy (Q_m) at a given ϵ, and the variable h is the sequence of simulations. If the variable ϵ changes in an interval, say $\epsilon = T \in (1, 2]$ or $r \in (0, 1]$, then $\omega_h(\epsilon, \cdot), \epsilon = T \in (1, 2]$ or $r \in (0, 1]$ represents a curve and $\omega_h(\epsilon), \epsilon = T \in (1, 2]$ or $r \in (0, 1]$ represents a family of curves. The final result $\varphi(\epsilon)$ is obtained by averaging over at least 100 of simulation results $\omega_h(\epsilon), \epsilon = T \in (1, 2]$ or $r \in (0, 1]$, i.e., $\varphi(\epsilon) = (\sum_{h=1}^{100} \omega_h(\epsilon, Q_1)/100, \ldots, \sum_{h=1}^{100} \omega_h(\epsilon, Q_m)/100), \epsilon = T \in (1, 2]$ or $r \in (0, 1]$. If strategies of all agents do not change for 1000 consecutive generations, it is deemed that a steady state has been reached and the iteration ends.

4 Results and discussion

Assume that there is a population of $N = 2\,500$ agents who occupy all nodes of a NW small-world network. For constructing the network, the probability that links are added between any two randomly chosen nodes is set at $p_{\rm nw} = 0.5$, and the number of nearest neighbors of each node is set at $k_{\rm nn} = 10$, if not otherwise explicitly stated. Throughout all simulations, the network topology remains static. In addition, the n-person PD and SD games are employed in simulations, respectively. To be compatible with previous studies and without loss of generality, the payoff matrix of a two-person PD game is chosen as $R = 1$, $1 < T \leq 2$, and $P = S = 0$ satisfying the inequality $T > R > P \geq S$, while the payoffs for n-person PD game will be calculated according to equation (2) satisfying the inequalities [40] given as follows

$$\begin{cases} P_C(n_c) > P_C(n_c - 1) \;\&P_D(n_c) > P_D(n_c - 1), \\ P_D(n_c) > P_C(n_c), \\ (n_c + 1)P_C(n_c) + (n - n_c - 1)P_D(n_c + 1) > \\ n_c P_C(n_c - 1) + (n - n_c)P_D(n_c). \end{cases} \tag{11}$$

The payoff matrix of the two-person SD game is chosen as $R = b - c/2$, $T = b \geq 1$, $S = b - c$ and $P = 0$ satisfying $T > R > S > P$, and the cost-to-benefit ratio is $r = c/b$, where $c = 1$ and $0 < r \leq 1$, while the payoffs for n-person SD game will be calculated according to equation (3). The n-person games are played according to the physical model in Section 2, and the payoffs of agents can be calculated by equation (8) or equation (9). Finally, an agent's strategy is updated with probability p, where the intensity of selection λ in equation (10) is set at $\lambda = 0.05$.

In this section, at first, how statistical results are obtained is described, and then the results are compared and analyzed, when the expected payoffs and the measured payoffs are used, respectively. Before each simulation starts, m strategies are randomly taken from the full quantum strategy space $\hat{S}$. After the model in Section 3 is iterated a large number of times, a simulation result is produced, $\omega_h(\epsilon), \epsilon = T \in (1, 2]$ or $r \in (0, 1]$. Also, because $\hat{S}$ is a very large space, in order to reduce randomicity, the final result, $\varphi(\epsilon), \epsilon = T \in (1, 2]$ or $r \in (0, 1]$, is obtained statistically by averaging 100 of simulation results, which is performed as follows. Suppose that there are 100 of

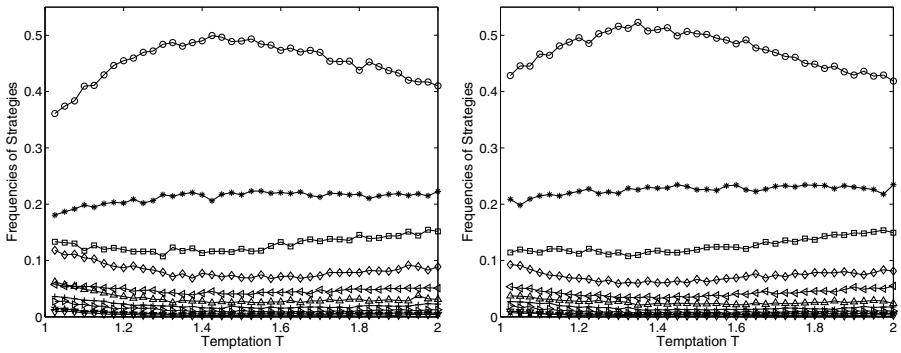

Fig. 3. The evolution of strategies when expected payoffs and measured payoffs are used. (a) Expected payoffs. (b) Measured payoffs. The figures that are drawn according to two final results $\varphi(\epsilon), T \in (1, 2]$, exhibit the fractions of agents with different strategies in a population of $N = 2\,500$ agents, when the expected payoffs and measured payoffs are used, respectively, in the 2×10 $(n = 2, m = 10)$ Prisoner's Dilemma (PD) games.

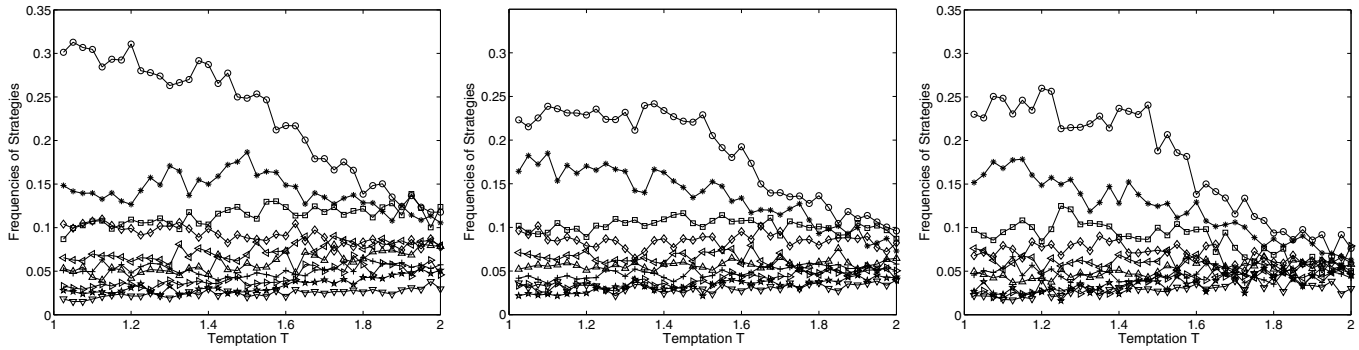

Fig. 4. The evolution of strategies when the number of initial strategies m rises. (a) $m = 30$. (b) $m = 40$. (c) $m = 50$. The figure exhibits the fractions of agents with different strategies after the $2 \times m$ $(n = 2, m = 30, 40, 50)$ Prisoner's Dilemma (PD) games are played 100 000 times in a population of $N = 2\,500$ agents at different m, in which only the first ten largest fractions are drawn because of low fractions of others.

simulation results $\omega_h(\epsilon), h = 1, 2, \ldots 100, \epsilon = T \in (1, 2]$ or $r \in (0, 1]$, each of which is a family of curves like one of Figures 2a–2c. Each point in these figures is the fraction of agents with a certain strategy at a given ϵ, $\omega_h(\epsilon, Q_m)$. In each figure, the strategy that produces the first (or topmost) curve is defined as Q_1, the second curve as Q_2, and so on. Thus, in terms of the method in Section 3, a statistical result is obtained, $\varphi(\epsilon), \epsilon = T \in (1, 2]$ or $r \in (0, 1]$, as is shown in Figure 3.

The model in Section 3 allows one to use expected payoffs or measured payoffs as the payoffs that agents receive after playing games. When a 2×10 $(n = 2, m = 10)$ PD game is adopted, there are four states $(|00\rangle, |01\rangle, |10\rangle, |11\rangle)$ in the superposition before measurement. Once the final state is measured, it will collapse to one of four states in the superposition with probability $|\langle \cdot | \psi_f \rangle|^2$, where $|\cdot\rangle$ represents one of four states. Thus, the first agent's payoffs at different states are $P(M(|\psi_f\rangle) = |00\rangle) = R$, $P(|01\rangle) = S$, $P(|10\rangle) = T$ and $P(|11\rangle) = P$. The statistical result of strategy evolution, $\varphi(T), T \in (1, 2]$, using expected payoffs and measured payoffs are shown in Figure 3. It can be seen that similar results are obtained, no matter which kind of payoffs are used. Hence, for reducing complexity, expected payoffs are used as agents' payoffs in the rest of the paper.

In Figures 3a–3b, we can see that there is a curve that is higher than others, i.e., the fraction of agents with a certain strategy is highest in the population and the strategy is also a dominant strategy. For the expected payoff case, it can be inferred that if higher payoffs can always be acquired when an agent uses a certain strategy against all strategies, then the strategy will be the dominant strategy in the end. As for the measured payoff case, it can be concluded that if the probability of collapsing to certain basic states in the final state $|\psi_f\rangle$ is high, and the agent can receive higher payoffs under that strategy profile corresponding to the basic state, finally the strategy will be the dominant strategy.

In addition, when the total number of agents N in the population remains constant, but the number of initial strategies m is increased, the evolution of strategies in $2 \times m$ PD games is shown in Figure 4. From Figure 4, it can be found that the fraction of agents adopting the dominant strategy in the population drops significantly, when

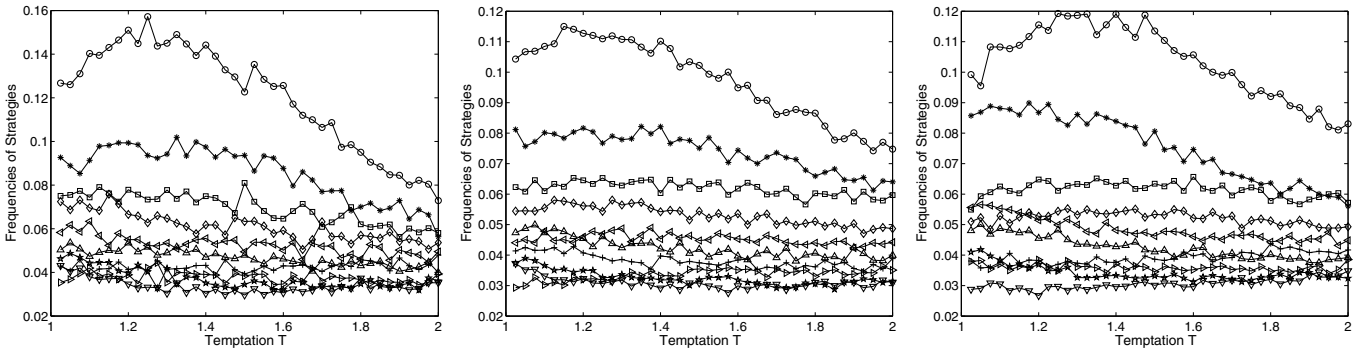

Fig. 5. The evolution of strategies in different sizes of populations at a given m. (a) $N = 5\,000$. (b) $N = 7\,500$. (c) $N = 10\,000$. The figure shows the fractions of agents with different strategies when N rises after the 2×50 ($n = 2, m = 50$) Prisoner's Dilemma (PD) games are played 100 000 ($N = 5\,000$ and $N = 7\,500$) and 150 000 ($N = 10\,000$) times, respectively, where only the first ten largest fractions of strategies are drawn because of low fractions of others.

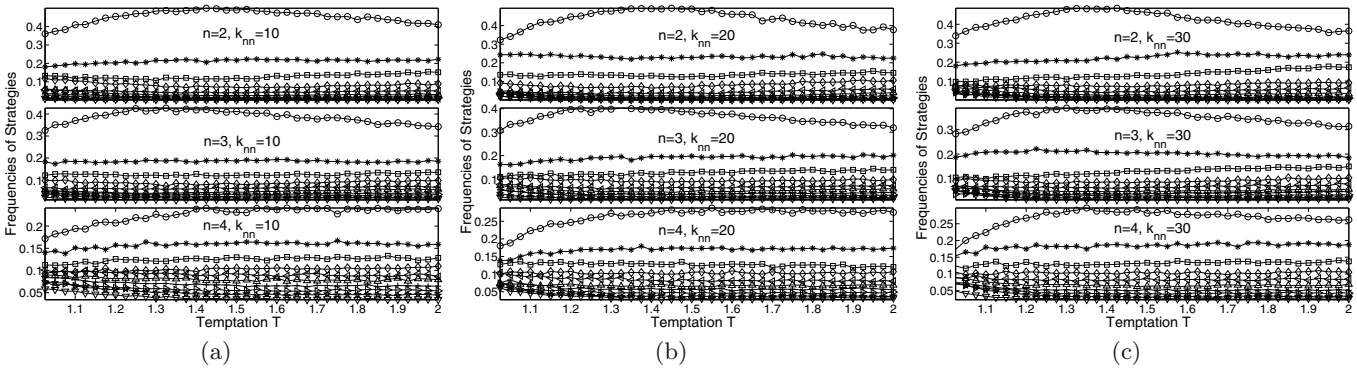

Fig. 6. The evolution of strategies at different n and $k_{\rm nn}$ when the Prisoner's Dilemma (PD) games are used. (a) $k_{\rm nn} = 10$. (b) $k_{\rm nn} = 20$. (c) $k_{\rm nn} = 30$. In the upper, middle and lower subfigures of (a), (b) and (c), the numbers of agents in a game are $n = 2, 3$ and 4, respectively. The results are obtained in a population of $N = 2\,500$ agents after the $n \times 10$ ($n = 2, 3, 4, m = 10$) PD games are played 50 000 times.

the variable T reaches a critical value. If T rises further, the dominant strategy almost disappears from the population. Comparing Figures 4a–4c, we can see that the critical value of T, at which the fraction of agents with the dominant strategy decreases largely when $m = 50$, is smaller than that when $m = 30$. Moreover, the fraction of agents with the dominant strategy at $T = 2$ when $m = 50$ is lowest among all cases. It can be inferred that after the initial strategies are assigned, the lower the initial fractions of agents with strategies in the population are, the earlier the dominant strategy disappears in the population. This can be regarded as a temporary "hibernation" of strategies because of the adverse environment, such as low fractions of initial strategies and a large T. However, once the disadvantageous conditions are removed, they will recover and one of them will become the dominant strategy again. In other words, if the total number of agents N in the population rises at a given m, even if other conditions remain the same, the dominant strategy will emerge in the population after the evolution comes to an end, as is shown in Figure 5. Therefore, we suggest that initially the number of agents with a certain strategy in the population is no less than 200. In the following simulations, for avoiding "hibernation" and saving simulation time, the number of strategies is set at $m = 10$ when $N = 2\,500$, so there are 250 agents adopting each strategy.

In the following part, when two different games are applied, the effects on the evolution of strategies are investigated and the relationships among the evolution, the number of players n in a n-person game, the number of nearest neighbors $k_{\rm nn}$ are discussed. Figures 6 and 7 exhibit the results of strategy evolution on small-world networks over the combinations of different conditions. From Figures 6 and 7, it can be seen that the fraction of agents using the dominant strategy in the population rises first and then remains relatively constant in a period of time, and finally drops slightly again as the variable T or r rises. Comparing two games, we can find that this rising-remaining-dropping process is clearer in the SD games than that in the PD games due to different payoff matrices. There is another reason for this phenomenon, namely, the different initial strategies. As is mentioned above, the full quantum strategy space is a very large space, so different initial quantum strategies can bring different results of evolution. As is shown in Figure 2, they are obtained from

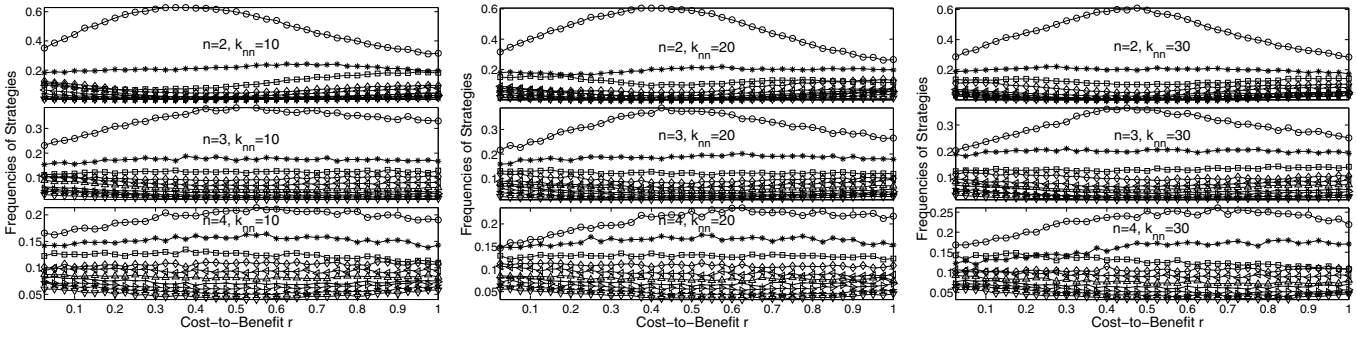

Fig. 7. The evolution of strategies at different n and $k_{\rm nn}$ when the Snowdrift (SD) games are used. (a) $k_{\rm nn} = 10$. (b) $k_{\rm nn} = 20$. (c) $k_{\rm nn} = 30$. In the upper, middle and lower subfigures of (a), (b) and (c), the numbers of agents in a game are $n = 2$, 3 and 4, respectively. The results are obtained in a population of $N = 2\,500$ agents after the $n \times 10$ ($n = 2, 3, 4, m = 10$) SD games are played 50 000 times.

three groups of initial strategies, in which the fraction of agents adopting the dominant strategy increases with the increase of the variable T in Figures 2a and in 2b it remains relatively stationary, whereas in Figure 2c it decreases with the increase of the variable T. If they are averaged statistically, two ends of the curve will drop, while the middle part will remain relatively stationary.

On the other hand, the fraction of agents adopting the dominant strategy decreases with the increase of the number of players n in a n-person game, when $k_{\rm nn}$ is constant, whereas the fractions are similar when $k_{\rm nn}$ rises and n remains constant. In fact, the number of items in a superposition will rise exponentially if n rises. For example, there are $2^4 = 16$ items in the superposition when $n = 4$, which causes expected payoffs drop. Moreover, as n rises, the number of groups l, into which the neighbors of an agent are divided, will reduce too, which makes the total payoffs of agents F decrease significantly. It is worse that the differences among agents' payoffs become smaller. As such, the probability p, with which an agent imitates the opponent's strategy, becomes smaller too, because it is a function of the difference of total payoffs. Figure 8 shows the averages and the standard deviation of payoffs of agents at different n and $k_{\rm nn}$, when the PD games are played. It can be seen that the averages and standard deviation of payoffs decrease with the increase of n, while the averages of payoffs are similar at the same n when $k_{\rm nn}$ rises.

Further, when two classical strategies are added into m strategies initially, the evolution of classical and quantum strategies on NW networks is investigated. As mentioned above, the set of classical strategies is a subset of the full quantum strategy set $\hat{S}$. Therefore, two classical strategies, Cooperation (C) and Defection (D), can also be taken from the space $\hat{S}$, which have the following forms

$$C = \hat{Y}(0,0,0) = \begin{pmatrix} 1 & 0 \\ 0 & 1 \end{pmatrix} \in \hat{S}$$

$$\text{and} \qquad D = \hat{Y}(0,0,\pi) = \begin{pmatrix} 0 & i \\ i & 0 \end{pmatrix} \in \hat{S}, \qquad (12)$$

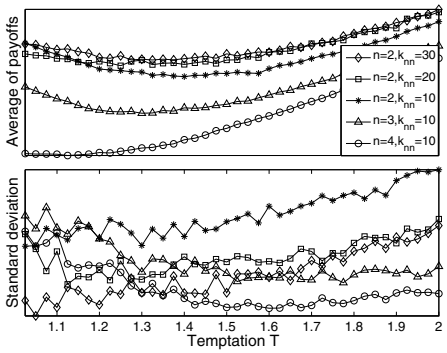

Fig. 8. The averages and the standard deviation of payoffs of agents at different n and $k_{\rm nn}$. The payoffs of $N = 2\,500$ agents are obtained after the $n \times 10$ ($n = 2, 3, 4, m = 10$) Prisoner's Dilemma (PD) games are repeated 50 000 times, when $n = 2$, 3, 4 and $k_{\rm nn} = 10$, 20, 30.

,

while the left $m-2$ strategies are still chosen from $\hat{S}$ at random, before each simulation starts. Later, the evolution of both classical and quantum strategies on the network is performed over different conditions. The final results of the evolution of classical and quantum strategies are respectively shown in Figures 9 and 10, in which the statistical results are obtained by the above mentioned method.

From Figure 9, it can be found that a quantum strategy defeats the classical strategies and becomes the dominant strategy when the PD game is employed. If the SD game is played, the classical strategy C has a chance to be the dominant strategy in the population, when the cost-to-benefit ratio r is small. However, as r rises, the fraction of agents with the strategy C drops constantly. On the contrary, a quantum strategy will become the dominant strategy, once r is larger than 0.3. When the number of agents n rises, a quantum strategy becomes the dominant strategy at a smaller r. On the other hand, the fractions of agents with the dominant strategy are similar with the increase of $k_{\rm nn}$ in both games. It is worth noting that the fraction of agents with the classical strategy D is always low, when quantum strategies are involved. Nevertheless, when only classical strategies, C and D, evolve on networks, finally

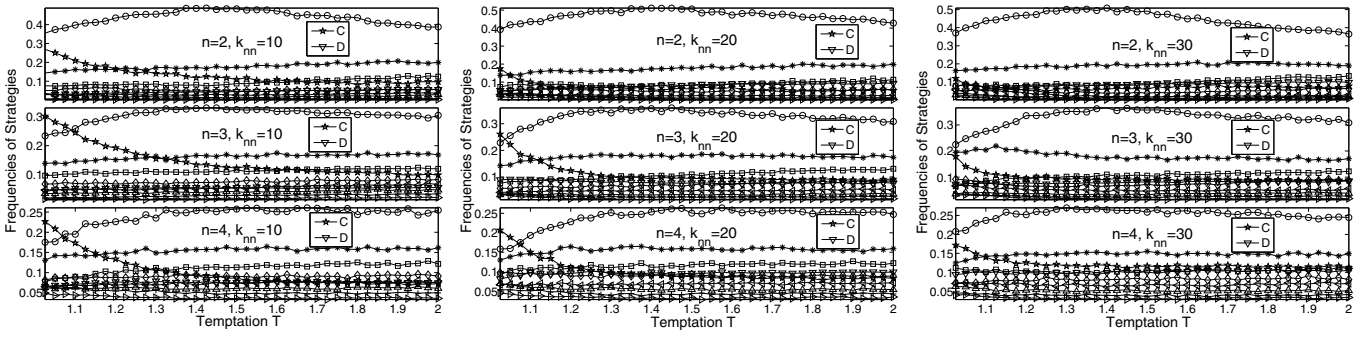

Fig. 9. The evolution of classical and quantum strategies at different n and $k_{\rm nn}$ when the Prisoner's Dilemma (PD) games are used. (a) $k_{\rm nn} = 10$. (b) $k_{\rm nn} = 20$. (c) $k_{\rm nn} = 30$. In the upper, middle and lower subfigures of (a), (b) and (c), the numbers of agents in a game are $n = 2$, 3 and 4, respectively. The results are obtained in a population of $N = 2\,500$ agents after the $n \times 10$ $(n = 2, 3, 4, m = 10)$ PD games are played 50 000 times.

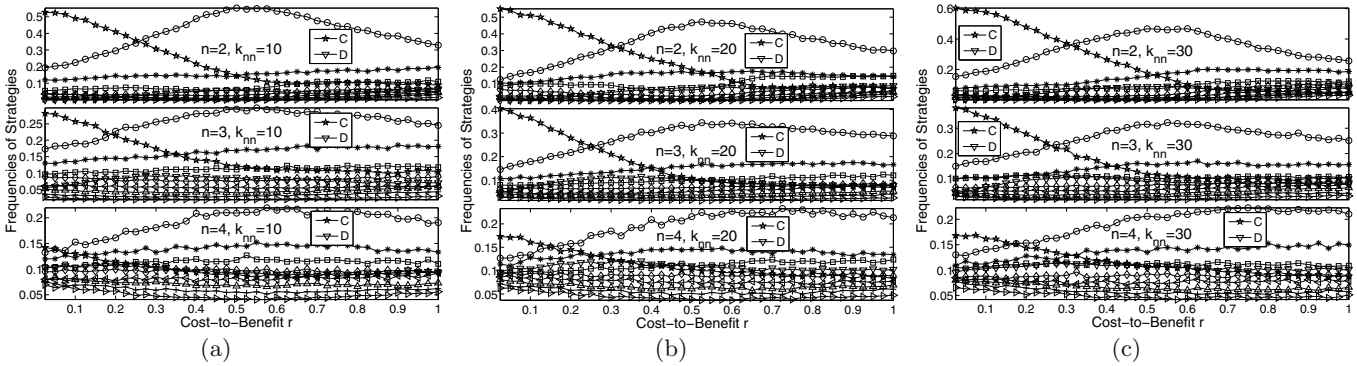

Fig. 10. The evolution of classical and quantum strategies at different n and $k_{\rm nn}$, when the Snowdrift (SD) games are used. (a) $k_{\rm nn} = 10$. (b) $k_{\rm nn} = 20$. (c) $k_{\rm nn} = 30$. In the upper, middle and lower subfigures of (a), (b) and (c), the numbers of agents in a game are $n = 2$, 3 and 4, respectively. The results are obtained in a population of $N = 2\,500$ agents after the $n \times 10$ $(n = 2, 3, 4, m = 10)$ SD games are played 50 000 times.

the strategy D always becomes the dominate strategy in the population. In conclusion, it is inferred that a quantum strategy can outperform the classical strategies.

5 Conclusions

In summary, the evolution of quantum strategies on a small-world network is investigated, in which quantum strategies are taken from the full quantum strategy space. As is known, the full quantum strategy space is a very large space and the classical strategy space is only a subset of it. Agents using strategies in $\hat{S}$ interact with their neighbors according to the physical model of a quantum game. When n-person PD and SD quantum games are employed, interesting results have been obtained over the combinations of different conditions.

In the statistical results, it can be seen that there exists a strategy that dominates the population, after the evolution of strategies comes to an end. Further, by analyzing the data, we can find that if higher expected payoffs are received by an agent who plays a certain strategy against all strategies, the strategy finally becomes the dominant strategy. On the other hand, if the total number of agents N in the population remains constant, while the number of initial strategies m rises, the fractions of agents with strategies will drop. In particular, the dominant strategy almost disappears in the population because of low fractions of initial strategies and a large T. However, once these disadvantageous conditions are removed, the dominant strategy will re-emerge in the population.

In addition, it can be found that the fraction of agents adopting the dominant strategy in the population decreases with the increase of the number of agents n in a n-person game that we consider. If both classical and quantum strategies evolve on the network, a quantum strategy can defeat the classical ones and prevail in the population.

This work is supported by the National Natural Science Foundation of China (Grant Nos. 61105125 and 51177177), by the China Postdoctoral Science Foundation (Grant No. 2011M501385) and by the Australian Research Council (Grant DP0771453).

References

1. M. Perc, A. Szolnoki, Biosystems **99**, 109 (2010)
2. G. Szabó, A. Szolnoki, R. Izsak, J. Phys. A **37**, 2599 (2004)
3. F.C. Santos, J.F. Rodrigues, J.M. Pacheco, Phys. Rev. E **72**, 056128 (2005)
4. L.H. Shang, X. Li, X.F. Wang, Eur. Phys. J. B **54**, 369 (2006)
5. F. Fu, L.H. Liu, L. Wang, Eur. Phys. J. B **56**, 367 (2007)
6. X. Chen, L. Wang, Phys. Rev. E **77**, 017103 (2008)
7. Q. Li, A. Iqbal, M. Chen, D. Abbott, Physica A **391**, 3316 (2012)
8. A. Eriksson, K. Lindgren, J. Theor. Biol. **232**, 399 (2005)
9. C.H. Chan, H. Yin, P. Hui, D.F. Zheng, Physica A **387**, 2919 (2008)
10. J.M. Pacheco, F.C. Santos, M.O. Souza, B. Skyrms, Proc. Roy. Soc. B: Biol. Sci. **276**, 315 (2009)
11. M. Ji, C. Xu, D.F. Zheng, P. Hui, Physica A **389**, 1071 (2010)
12. P.E. Turner, L. Chao, Nature **398**, 441 (1999)
13. T. Pfeiffer, S. Schuster, S. Bonhoeffer, Science **292**, 504 (2001)
14. T. Frick, S. Schuster, Naturwissenschaften **90**, 327 (2003)
15. C. Chettaoui, F. Delaplace, M. Manceny, M. Malo, Biosystems **87**, 136 (2007)
16. D.A. Meyer, Phys. Rev. Lett. **82**, 1052 (1999)
17. J. Eisert, M. Wilkens, M. Lewenstein, Phys. Rev. Lett. **83**, 3077 (1999)
18. L. Marinatto, T. Weber, Phys. Lett. A **272**, 291 (2000)
19. A. Iqbal, A.H. Toor, Phys. Lett. A **280**, 249 (2001)
20. R. Kay, N.F. Johnson, S.C. Benjamin, J. Phys. A **34**, L547 (2001)
21. J. Du, H. Li, X. Xu, M. Shi, J. Wu, X. Zhou, R. Han, Phys. Rev. Lett. **88**, 137902 (2002)
22. R. Prevedel, A. Stefanov, P. Walther, A. Zeilinger, New J. Phys. **5**, 205 (2007)
23. C. Schmid, A.P. Flitney, W. Wieczorek, N. Kiesel, H. Weinfurter, L.C.L. Hollenberg, New J. Phys. **12**, 063031 (2010)
24. A. Iqbal, A.H. Toor, Phys. Lett. A **300**, 541 (2002)
25. A. Iqbal, A.H. Toor, Phys. Lett. A **293**, 103 (2002)
26. J.M. Chappell, A. Iqbal, D. Abbott, PLoS ONE **6**, e21623 (2011)
27. J.M. Chappell, A. Iqbal, D. Abbott, PLoS ONE **7**, e29015 (2012)
28. J.M. Chappell, A. Iqbal, D. Abbott, PLoS ONE **7**, e36404 (2012)
29. A.P. Flitney, D. Abbott, Fluct. Noise Lett. **2**, R175 (2002)
30. H. Guo, J. Zhang, G.J. Koehler, Decis. Support Syst. **46**, 318 (2008)
31. A. Ekert, P.M. Hayden, H. Inamori, Coherent Atomic Matter waves **72**, 661 (2001)
32. D. Deutsch, R. Jozsa, Proc. Roy. Soc. Lond. Ser. A, Math. Phys. Sci. **439**, 553 (1992)
33. M.A. Nielsen, I.L. Chuang, *Quantum Computation and Quantum Information* (Cambridge University Press, Cambridge, 2000)
34. S.C. Benjamin, P.M. Hayden, Phys. Rev. A **64**, 030301 (2001)
35. J. Du, H. Li, X. Xu, M. Shi, X. Zhou, R. Han, Arxiv: quant-ph/0111138 (2001)
36. M.E.J. Newman, D.J. Watts, Phys. Rev. E **60**, 7332 (1999)
37. M.E.J. Newman, D.J. Watts, Phys. Lett. A **263**, 341 (1999)
38. M.E.J. Newman, SIAM Rev. **45**, 167 (2003)
39. G. Szabó, C. Toke, Phys. Rev. E **58**, 69 (1998)
40. R. Boyd, P.J. Richerson, J. Theor. Biol. **132**, 337 (1988)